J Mol Model (2016) 22: 17
DOI 10.1007/s00894-015-2886-8

ORIGINAL PAPER

DFT investigation on dihydrogen-bonded amine-borane complexes

Shihai Yan[1] · **Hongmei Zou**[2] · **Wukui Kang**[1] · **Lixiang Sun**[3]

Received: 1 September 2015 / Accepted: 10 December 2015 / Published online: 22 December 2015

Abstract The DFT method has been employed in the exploration on dihydrogen-bonded amine-borane complexes, with a special emphasis on the dimerization and substituent group effect. Stable dihydrogen bonded complexes can be generated from these amine-borane monomers with the appearance of $NH^{\delta+}\ldots H^{\delta-}B$ interactions. The binding energy decreases gradually with the increase of the steric effect of the substituents. The substituent group number mainly varies the C-N bond length. The dimerization generates close H…H and influences predominantly the N-B distance. The effect of dimerization on IR and vibrational circular dichroism (VCD) spectra is stronger than that of the number of substituent groups, which leads to distinct NBO charge variation on α-C. Both the substituent group number and dimerization enhance the chemical shift difference between hydrogen atoms covalently bonded to N and B, $\Delta\delta_{H\text{-}H}$, which can be hired as an index for structural determination. It is proposed that amine-borane complexes with more substituent groups in higher degree of polymerization are potentially interesting materials for hydrogen storage.

Keywords Amine-borane · Dihydrogen bond · Dimerization · NMR parameters · Substituent group

Hongmei Zou and Wukui Kang contributed equally to this work.

✉ Shihai Yan
yansh@qibebt.ac.cn; shyan@qau.edu.cn

[1] Present address: College of Chemistry and Pharmaceutical Sciences, Qingdao Agricultural University, Qingdao 266109, China

[2] College of Food Science and Engineering, Qingdao Agricultural University, Qingdao 266109, China

[3] College of Chemistry and Materials Science, Ludong University, Yantai 264025, China

Abbreviations

DFT	density functional theory
DBAB	α-dimethylbenzyl amine-borane
DHB	dihydrogen bond
DSO	diamagnetic spin-orbit
EAB	ethylamine-borane
E_b	binding energy
FC	Fermi contact
GIAO	gauge independent atomic orbital
HB	hydrogen bond
IR	infrared
MAB	methylamine-borane
MBAB	α-methylbenzyl amine-borane
NBO	natural bond orbital
NMR	nuclear magnetic resonance
PSO	paramagnetic spin-orbit
SD	spin dipole
TMS	tetramethylsilane
VCD	vibrational circular dichroism

Introduction

Hydrogen bond (HB) formation induces variations of the structure of the interacting molecules. These changes regulate the structure and function of biological molecules, and is responsible for the properties of materials and molecular assembly. A novel type of HB was identified in the middle 1990s [1, 2]. It is designated as X-H…H-Y (where X-H is the typical proton donating group and Y refers to a transition metal or boron), and has inspired extensive efforts to characterize its unique features. This type of interaction is termed as dihydrogen bond (DHB) owing to the H…H contact between the coupled pairs [3]. It is pivotal to harness the DHB to promote chemical reactivity and

selectivity just as nature uses the classical HB in enzymatic catalysis. This field will challenge our still limited ability to design molecules with useful and tunable catalytic properties.

Crabtree and coworkers brought out 26 systems with short H…H contacts (<2.2 Å) [3] based on a comprehensive survey of the Cambridge Structural Database (CSD). The dihydrogen bonded aza-borane derivatives show similar cooperativity to those observed in standard HBs [4]. The electron bridging DHB has been found in imidazole involved derivatives, which is described from the geometrical structure, the highest occupied molecular orbital, the NMR parameters, and the stabilization energy viewpoint [5]. The H…H distances in DHB are in the range of 1.7–2.2 Å. The N-H…H angle ranges around 160° with an amplitude of 10°, and the B-H…H angle tends to be more bent than linear. The nature of X-H…H-Y DHB is described theoretically for simple model systems [6]. The primary features for this interaction are the close distance between two hydrogen atoms, the absence of lone pair repulsion, and the high polarizability of the Y-H bond. The most significant energetic terms are attributed to the electrostatic and exchange contributions.

Nowadays, a great challenge is to move toward a hydrogen-based energy economy through the search for safe, economical, and hydrogen-rich materials. As potential

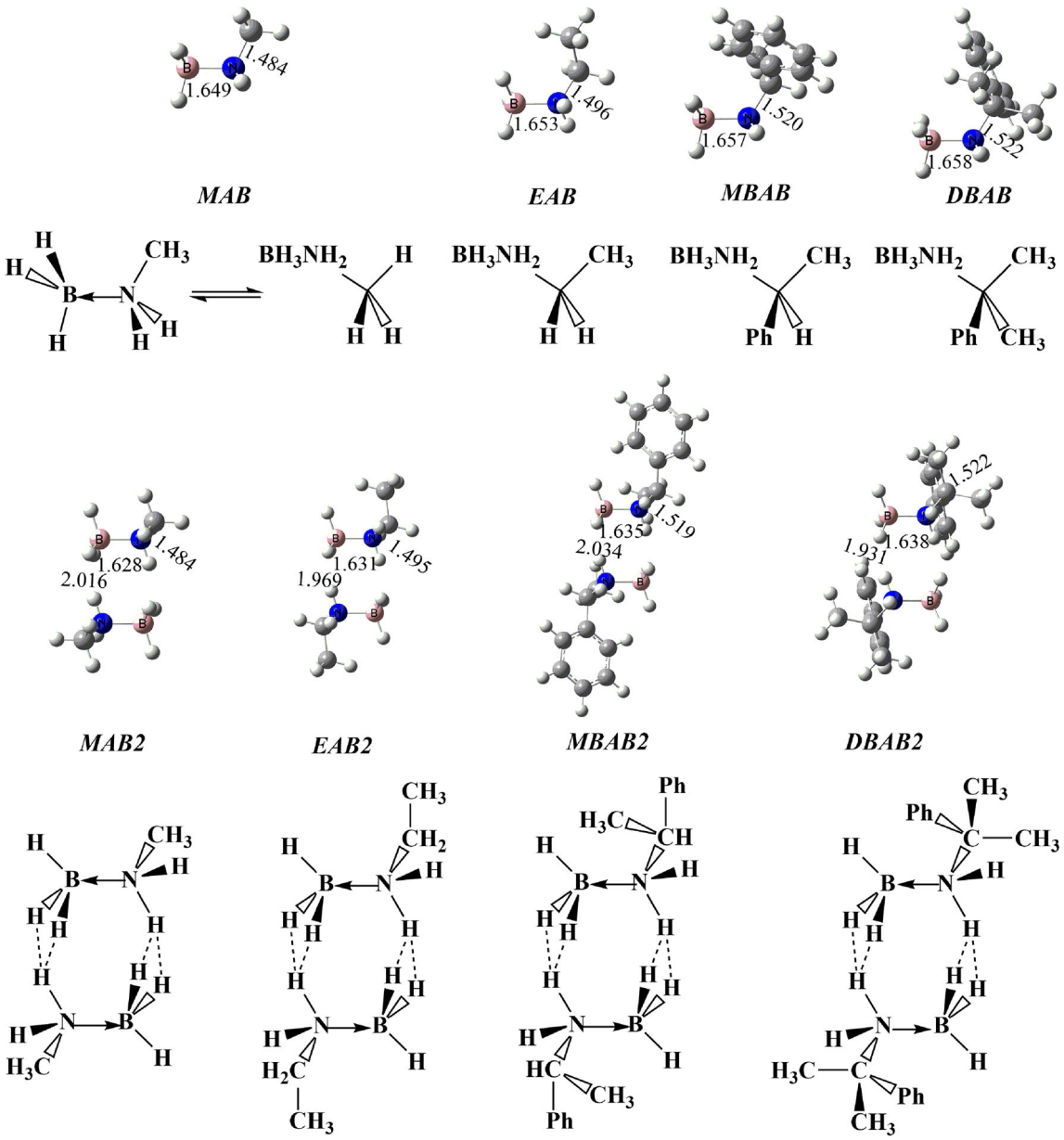

Fig. 1 Geometry structures with the primary bond lengths of the amine-borane complexes

hydrogen storage materials or dehydrogenation catalysts, ammonia-borane and related compounds have generated extensive excitement [7, 8]. The DHB has been observed in such amine-borane complexes [8–10]. X-ray crystallography has been utilized in structural studies, where a DHB is identified by an average H…H distance of 1.96 Å, an average N-H…H angle of 150°, and an average B-H…H angle of 120° in the N-$H^{\delta+}$…$H^{\delta-}$-B type interactions [3]. It was shown that the most stable conformation of $(H_3NBH_3)_2$ is a head-to-tail structure with two sets of bifurcated DHBs [11]. As the booming hydrogen storage candidates, the ammonia-boranes have the following merits: high hydrogen capacity, encouraging dehydrogenation performance, tunable hydrogen storage properties, and lasting stability in air [12]. It is pointed out that the strong DHB stabilizes the layered ammonia-borane structure and promotes the reaction between $H^{\delta+}$ and $H^{\delta-}$ and thus accelerates the release of dihydrogen at much lower temperature and faster rate. The DHB mediated alcoholysis of dimethylamine-borane in nonaqueous media has been explored both experimentally and theoretically [13].

DHBs can be detected indirectly using IR and NMR spectroscopy by monitoring the change of characteristic vibrational frequencies or ^{1}H chemical shifts. Very little further experimental IR data of DHBs has been reported since the first IR spectroscopy of DHB was reported in the 1970s [14–16]. The main limitation is due to the signal contamination of DHB by other HB interactions in solution. The vibrational circular dichroism (VCD) and NMR spectroscopy are highly sensitive to conformational variations and environmental turbulence, and have thus been employed successfully to identify the DHB of chiral amine-borane complex [17].

Herein, these three tools are hired to identify dihydrogen bonded dimers of amine-borane and its derivatives. The results and discussion about the geometrical structure, IR and VCD spectra, NBO charge, NMR, as well as the coupling mechanism are presented in this article. Concluding and opening remarks are also presented.

Calculation details

The high precision and computationally inexpensive performances exhibited by the hybrid B3LYP method lead to its extensive application, especially for the description of large free radicals, intermolecular complexes, and anions [18–23]. Although the B3LYP functional predicts a larger binding energy as compared with the MP2 method [24–26], the B3LYP functional gives data whose accuracy matches those of the best ab initio results. The B3LYP functional has been suggested efficient in the exploration [27–29] of the NMR spin-spin coupling constant (^nJ(A, B), where n is the number of bonds connecting nuclei A and B). The NMR calculations were performed employing the gauge independent atomic orbital (GIAO) framework [30, 31]. Tetramethylsilane (TMS) was utilized as the reference molecule. The J constants are determined as the sum of four Ramsey terms: the Fermi contact (FC: the magnetic interaction between an electron and an atomic nucleus when the electron is inside the nucleus), the spin dipole (SD), the paramagnetic spin-orbit (PSO), and the diamagnetic spin-orbit (DSO) contributions [32].

All calculations throughout this article were carried out employing the B3LYP exchange-correlation functional with the 6-311++G(d,p) basis set implemented in a suite of Gaussian 09 program package [33]. The absence of imaginary frequency in the vibrational spectra ensured that all the optimized structures were local minima on the potential energy surfaces. The binding energy (E_b) was calculated by subtracting the energies of monomers from that of the polymer.

Generally, the charges obtained from natural population analysis is more reliable than the Mulliken charges, especially, when the diffusion function is included. The charge distribution and the bonding feature of the polymers are revealed with the analysis on molecular orbital and natural bond orbital (NBO) [34]. According to the second-order perturbation theory, the orbital interactions between the donor (Lewis basic type) orbitals and the acceptor (Lewis

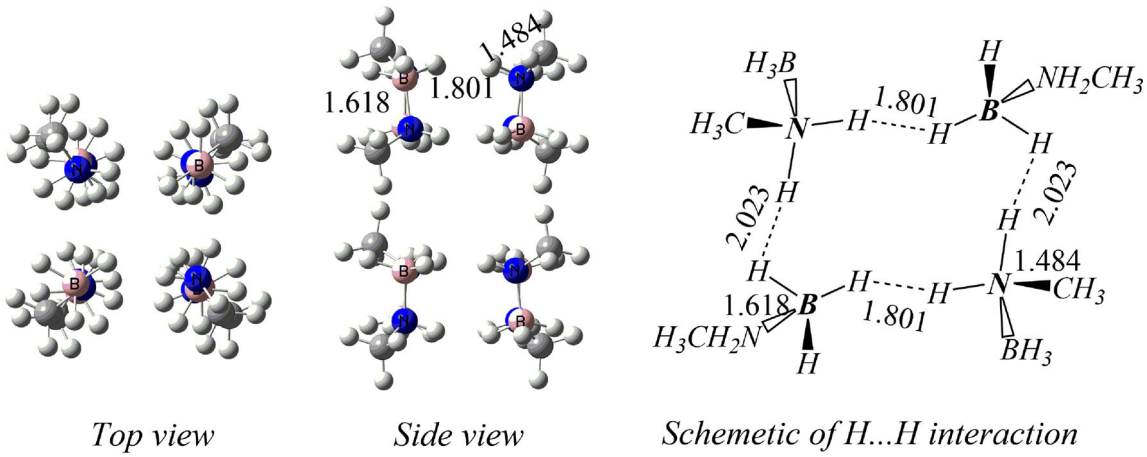

Fig. 2 Geometry structure of the amine-borane octamer (*MAB8*)

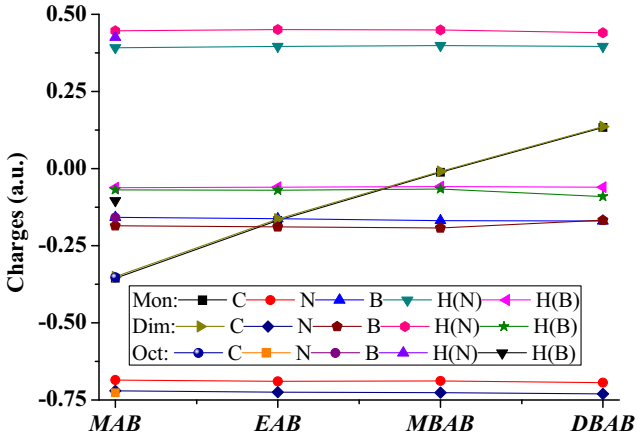

Fig. 3 Charge population on selected atoms of various amine-borane complexes. Mon means the monomer, Dim refers to the dimer, and Oct denotes the octamer. C is the atom bonded directly with N. H(N) and H(B) are the hydrogen atoms that participate in the H…H interaction in the polymer, respectively

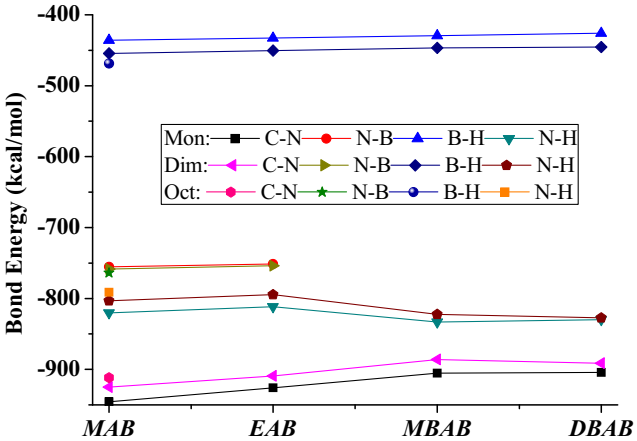

Fig. 5 Bond energies of primary bonds of various amine-borane complexes. Mon means the monomer, Dim refers to the dimer, and Oct denotes the octamer. Both N-H and B-H participate in the H…H interaction in the polymer

acidic type) orbitals are estimated. For each NBO donor orbital (i) and acceptor orbital (j), the stabilization energy $E(2)$ associated with the delocalization $i \rightarrow j$ is given by the formula:

$$E(2) = \Delta E_{ij} = q_i \frac{F(i,j)^2}{\varepsilon_j - \varepsilon_i}$$

,where q_i is the donor orbital occupancy, F(i, j) is the offdiagonal NBO Fock matrix element. εi and εj are diagonal elements (orbital energies).

Results and discussion

Geometries Figure 1 collects the optimized geometries of methylamine-borane (*MAB*), ethylamine-borane (*EAB*), α-

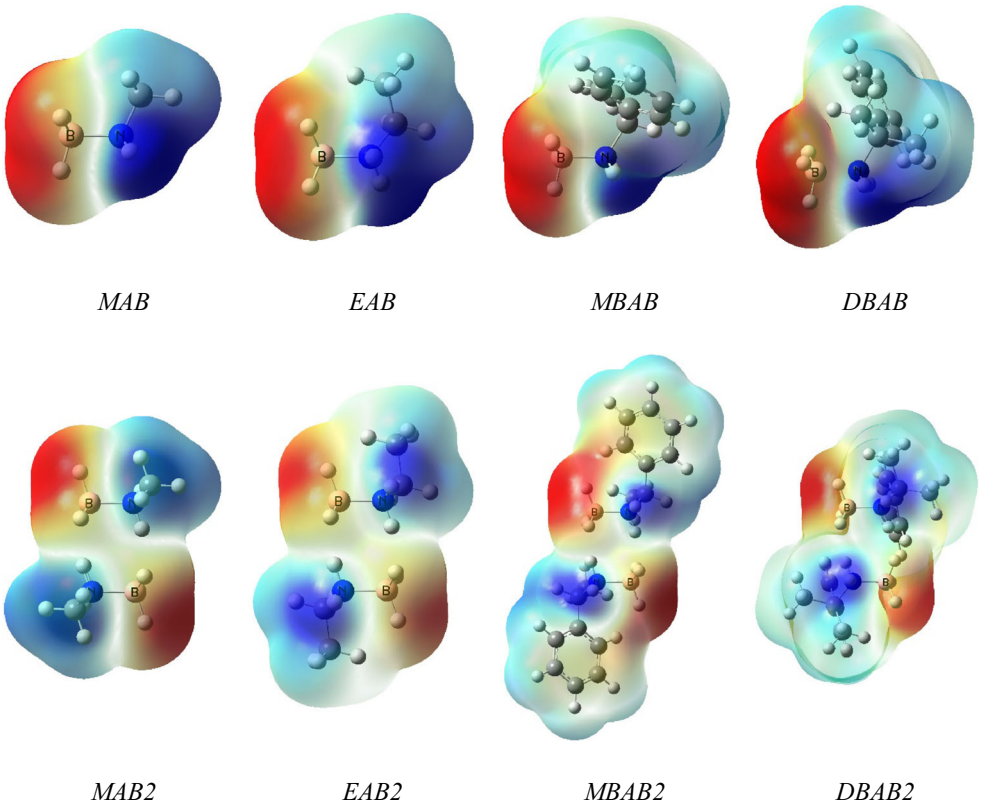

Fig. 4 Electrostatic potential of the amine-borane complexes. The blue surface denotes the positive part of the electrostatic potential, and the red area represents the negative part

Table 1 The stabilization energy E(2) in the dihydrogen-bonded amine-borane complexes

Complex	Donor	Acceptor	E(2) [a]
MBAB	LP of N [b]	LP* of B [c]	267.2
DBAB	LP of N	LP* of B	266.8
MBAB2	LP of N	LP* of B	289.2
DBAB2	LP of N	LP* of B	287.8

[a] The unit of E(2) is kcal mol^{-1} ; [b] LP means lone pair bond; [c] LP* denotes lone pair antibond of B

methylbenzyl amine-borane (*MBAB*), α-dimethylbenzyl amine-borane (*DBAB*), as well as the corresponding dimers (*MAB2*, *EAB2*, *MBAB2*, and *DBAB2*). The octamer of methylamine-borane (*MAB8*) is presented in Fig. 2. Each dimer has a head-to-tail structure with two sets of bifurcated DHBs, similar to that of $(H_3NBH_3)_2$ [11]. The primary parameters shown in this figure afford the following information. The C-N bond lengthens along with the number of substituent group on α-C, implying the weakening of the C-N bond. This is supported by the analysis about the bonding energy discussed later. Similarly, the distances of N-B, N-H, and B-H bonds increase slightly as the substituent group number augments. The N-B bond distance in *DBAB* is still slightly shorter than that (1.665 Å) in H_3NBH_3. Dimerization generates novel H…H interactions with short contact distance (~2.0 Å), as has been observed experimentally in *MBAB2* by VCD spectroscopy [17], and condenses the NB bond by ~0.02 Å for all four monomers. The effect of dimerization on other geometrical parameters is slight. The influence of polymerization on geometry is further explored with the optimization about the octamer of *MAB*. The N-B bond decreases in *MAB8* by 0.01 Å as compared to that in *MAB2*. The shortest H…H distance (1.801 Å) is observed in this octamer. The distance of N-H…H-B interaction is distinctly condensed as compared with those observed in amine-borane complexes [35–38], where the DHBs are generated by the $H^{\delta+}…H^{\delta-}$ interaction, which is generally shorter than those formed with the $H^{\delta+}…e…H^{\delta+}$ interaction [5, 39]. Therefore, the addition of substituent group mainly influences the C-N bond length. The augmentation of degree of polymerization generates close H…H contacts and varies predominantly with the original N-B distances. It is expected that the cooperation between ambient $H^{\delta+}…H^{\delta-}$ interactions provides the driving force for closer H…H contacts and shorter N-B bonds (1.618 Å).

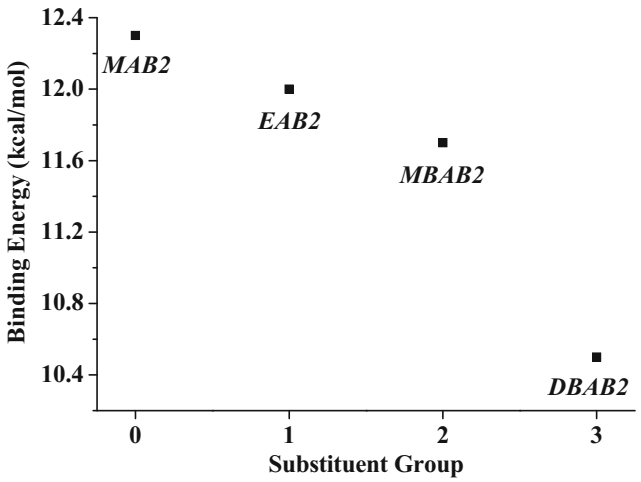

Fig. 6 Binding energies (E_b) of the dimers calculated at B3LYP/6-311++G(d,p) level

NBO analysis The NBO charge population on primary atoms of the amine-borane complexes are shown in Fig. 3. The NBO

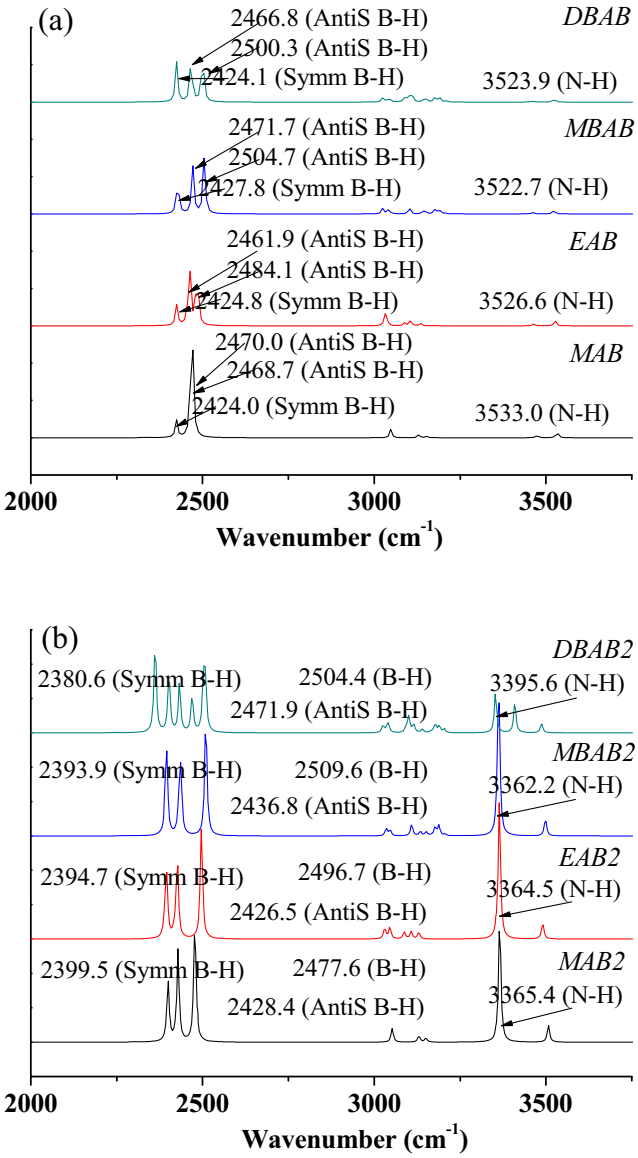

Fig. 7 IR spectra of amine-borane systems. The primary vibrational modes are assigned

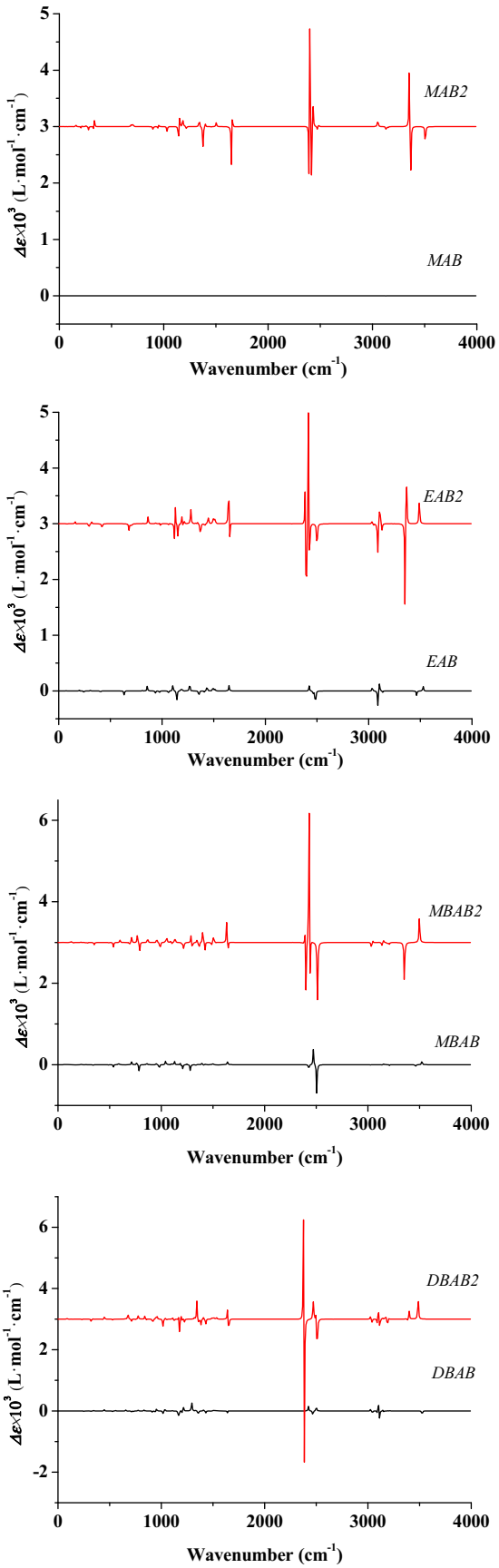

Fig. 8 The VCD spectra of amine-borane complexes

charges on α-C, N, and B atoms of *MAB* are −0.36, −0.69, and −0.16 atomic unit (a.u.), respectively. Positive charges of 0.39 a.u. and negative charges of −0.06 a.u. are found on the hydrogen atoms covalently bonded to N and B, respectively, and this indicates that the interaction mode of DHB in these dimers should be N-$H^{\delta+}$…$H^{\delta-}$-B. The charge on α-C varies gradually from negative to positive (0.13 a.u.) along with the increase of the substituent group number, the effect of which is slight on the charge population of other atoms. The charge population in the dimer is similar to those in the monomer, as is applicable to all four amine-borane complexes. This demonstrates that the influence of dimerization is weak on charge populations. This is supported by the charge population in *MAB8* (Fig. 3).

The molecular electrostatic potential (ESP) of these amine-borane complexes are shown in Fig. 4. Useful information about the charge population can also be obtained from these diagrams. The red-color surface denotes the negative electrostatic zone, and the blue-color part refers to the positive electrostatic area. Therefore, electronegative borane group combines with the electropositive amine group during the dimerization reaction. In the dimer, the positive area and the negative surface of the ESP are crisscrossed, and the system is stabilized by the cooperation of these electrostatic attractions.

The energies of primary bonds are represented in Fig. 5. The energies of the C-N, N-B, N-H, and B-H covalent bonds in *MAB* are −945.7, −755.3, −820.1, and −435.7 kcal mol^{-1}, respectively. The N-B bond energy (E_{NB}) is less by 27.4 kcal mol^{-1} as compared with that of H_3NBH_3. The value of E_{NB} decreases by 4.0 kcal mol^{-1} when one substituent group is added on α-C. The N-B covalent bond disappears in *MBAB* and *DBAB* complexes. Instead, the delocalization from the N lone pair (occupied) to the B lone pair antibond (virtual) contributes by 267.2 kcal mol^{-1} to the stabilization energy *E*(2) of

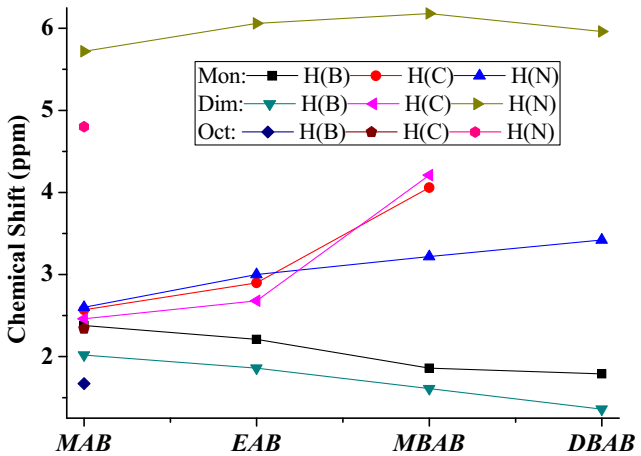

Fig. 9 Chemical shifts of primary hydrogen atoms in various amine-borane complexes. Mon means the monomer, Dim refers to the dimer, and Oct denotes the octamer. H(C) denotes the hydrogen aatom on α-C. H(N) and H(B) are the hydrogen atoms participate in the H…H interaction in the polymer, respectively

MBAB. This value reduces slightly to 266.8 kcal mol^{-1} in *DBAB* (Table 1). The E_{CN} value decreases slightly with the increase of the substituent group number. It is similar in the case of E_{BH}, which reduces linearly by ~3.0 kcal mol^{-1} step by step. The situation of E_{NH} is complex owing to the disappearance of N-B covalent bonds in *MBAB* and *DBAB* complexes. This leads to the strengthening of N-H interaction. E_{NH} decreases distinctly with the augmentation of degree of polymerization. The N-B covalent bond also disappears in the dimers of *MBAB* and *DBAB* complexes. The delocalization of the N lone pair to B contributes by 289.2 and 287.8 kcal mol^{-1} to *E*(2) of *MBAB2* and *DBAB2*. This phenomenon indicates that the dimerization effect on the property of the monomer is slight. This is proven by the slight difference between the bond energies of the octamer and monomer of *MAB* (Fig. 5).

The binding energy (E_b) of 15.1 kcal mol^{-1} for the related $(H_3NBH_3)_2$ has been predicted by Cramer [11]. The E_b of $(H_3NBH_3)_2$ determined at the B3LYP/6-311++G(d,p) level is 12.9 kcal mol^{-1}, in good accordance with the previously reported value. The dimerization of *MAB* is an exothermic reaction by 12.3 kcal mol^{-1}. The E_b value of *MAB2*, *EAB2*, *MBAB2*, and *DBAB2* calculated at the same level is 12.3, 12.0, 11.7, and 10.5 kcal mol^{-1}, respectively (Fig. 6). The E_b of 8.8 kcal for *MBAB2* has been predicted at the B3LYP/6-31G(d) level [17]. The decrease of E_b along with the augmentation of substituent group number should be attributed to the steric effect. The E_b value of 75.5 kcal mol^{-1}, predicted for *MAB8*, indicates that the binding strengthens with the cooperation of peripheral $H^{\delta+}\ldots H^{\delta-}$ interactions.

IR spectra IR spectroscopy is an invaluable tool in chemistry, material, and biological structure determination. It is sensitive to the bond order, the type of atoms joined by the bond, as well as the chemical environment. The IR spectra of the amine-borane complexes over a range of 2000 cm^{-1} are collected in Fig. 7, with the primary vibrational modes of strong intensity assigned. The spectra at 2424.0 and 2468.7 cm^{-1} are assigned as the symmetrical and anti-symmetrical B-H bonds stretching of *MAB* complex, respectively. The frequencies locating at 3533.0 cm^{-1} correspond to the N-H stretching mode, which is red-shifted by 27 cm^{-1} as compared to that in H_3NBH_3. The effect of the substituent group number on anti-symmetrical B-H stretching modes is distinct (Fig. 7 (a)). The spectra of two anti-symmetrical B-H stretching modes approach each other and they are degenerated owing to the similarity of chemical environment. These two spectra shift away gradually in the derivatives (*EAB*, *MBAB*, and *DBAB*) because the substituent groups change the chemical environment of two B-H bonds. Figure 7 indicates that the effect of the substituent group number is slight on these hydrogen bond stretching modes. Red-shift occurs upon dimerization for the symmetric B-H and N-H stretching modes, as can be observed obviously for all four monomers (Fig. 7b).

Vibrational circular dichroism (VCD) spectra As a powerful method to probe the binding topology of DHB systems, VCD spectra have been utilized both for the determination of absolute configurations and for structural studies of a wide range of systems ranging from small molecules to polymers [40–43]. The VCD spectra of the monomer and dimer complexes are shown in Fig. 8. The B-H stretching vibration is assigned in the VCD bands of *MAB* at 2468.7 cm^{-1}. It is in good agreement with the experimental results observed by Merten [17]. The intensity of this band is strengthened by a thousand times and it shifts to 2399.5 cm^{-1} upon dimerization. Another vibration with strong intensity of *MAB2*, located at 3353.9 cm^{-1}, corresponds to the N-H stretching vibration. The following two points can be drawn with the analysis about the VCD spectra of *EAB*, *MBAB*, *DBAB*, as well as their dimers expressed in the other three plots of Fig. 8. Firstly, a distinct VCD band, found around 2450 cm^{-1} for all three monomers, corresponds to the B-H stretching vibration. It is red-shifted upon dimerization slightly. Secondly, the typical signal at ~3500 cm^{-1} is assigned to the N-H stretching mode, which is red-shifted slightly upon dimerization, while the intensity is strengthened distinctly.

NMR parameters The sensitivity of NMR parameters to structure and environment provides a useful tool for structural identification. The chemical shift (δ) and spin-spin coupling constant (*J*) are important NMR parameters and offer detailed information on the geometry and electronic structures. The δ and *J* values are collected in Figs. 9 and 10, respectively. The following three points can be drawn from Fig. 9. Firstly, the increase substituent group number enhances the δ value of H, which is covalently bonded with α-C or N. The situation is opposite for the H covalently bonded with B. Secondly, the dimerization effects are predominant on the δ of nitric H (H(N)). Thirdly, the δ difference of H(N) and H(B), $\Delta\delta_{H\text{-}H}$, increases with the number of substituent groups from 0.22 to 1.63 ppm for the monomer and from 3.7 to 4.6 ppm for the dimer, respectively. This can be employed to detect the corresponding geometry structure.

Figure 10 demonstrates that the spin-spin coupling constants of B-H (J_{BH}) of both monomer and dimer are dominated predominantly by the Fermi-contact (FC) mechanism. The value of J_{BH} varies slightly with the addition of a substituent group. While, J_{BH} reduces distinctly by ~6.0 Hz upon dimerization. J_{NH} is determined mainly by the FC mechanism. A small contribution comes from the paramagnetic spin-orbit (PSO) mechanism of J_{NH}. The J_{NH} coupling constant varies slightly along with both the number of substituent groups and the dimerization. The coupling constant of N-B in the monomer is about 1.4 Hz and changes slightly vs substituent group number. J_{NB} is exalted by two times upon dimerization. The J_{CN} coupling constant is altered mainly vs the substituent group number, instead of the dimerization.

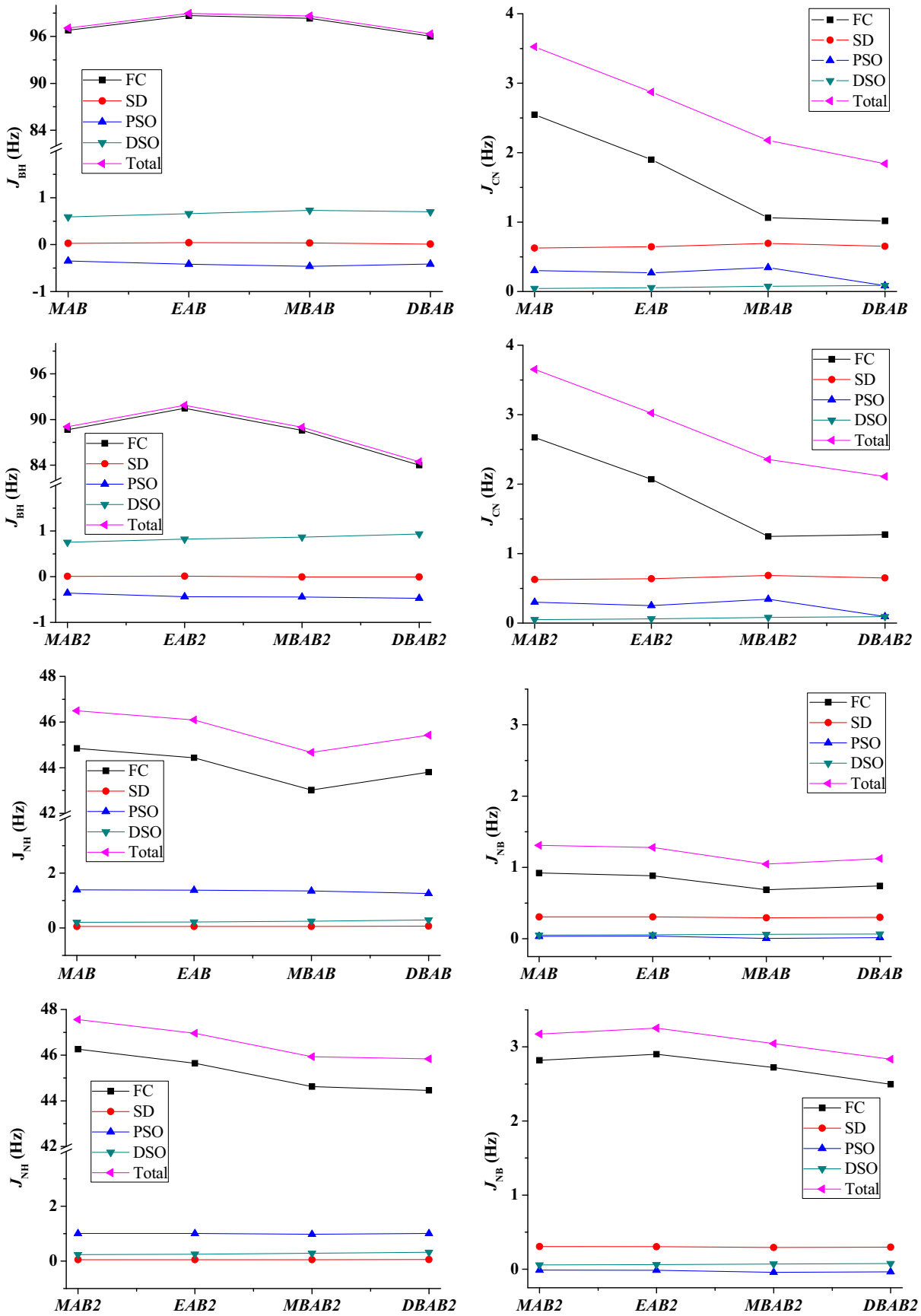

Fig. 10 The NMR spectra of amine-borane complexes. Both N-H and B-H participate in the H…H interaction in the polymer

Conclusions

The analyses of the geometrical structure, NBO charge, IR and VCD spectra, binding energy, and NMR parameters of the amine-borane complexes were performed on the basis of DFT results. Stable dihydrogen bonded complexes can be generated from these amine-borane monomers through N-$H^{\delta+}$…$H^{\delta-}$-B interactions upon polymerization. The binding energy of the dimer decreases gradually with the increase of the substituent group number at α-C owing to the steric effect. The number of substituent groups mainly influences the C-N length and the dimerization predominantly influences the N-B distance. The effect on IR and VCD spectra of dimerization is stronger than that of the number of substituent groups, which leads to distinct NBO charge variation on α-C. Both the number of substituent groups and dimerization enhance the chemical shift difference of hydrogen atoms covalently bonded to N and B, $\Delta\delta_{H\text{-}H}$, which can be hired as an index for the structural determination.

The stability of the system decreases with the addition of substituent group, while it is favorable for the release of hydrogen. The larger the degree of polymerization, the higher the stability. This would benefit the storage of dihydrogen. Therefore, the amine-borane complexes with more substituent groups in higher polymerization degree are expected to be excellent potential candidates for dihydrogen storage.

Acknowledgments This work is supported by National Nature Science Foundation of China (Grant No. 21203227, 21103080) and the Research Foundation for Talented Scholars of the Qingdao Agricultural University (No. 631335). The numerical calculations in this paper have been done on the supercomputing system in the Supercomputing Center of University of Science and Technology of China.

Author contributions The manuscript was written through contributions of all authors. All authors have given approval to the final version of the manuscript.

References

1. Park S, Ramachandran R, Lough AJ, Morris RH (1994) A new type of intramolecular H…H…H interaction involving N-H…H(Ir)…H-N atoms. Crystal and molecular structure of [IrH(η^1-$SC_5H_4NH)_2$(η^2-SC_5H_4N)(PCy_3)]BF_4·0.72CH_2Cl_2. J Chem Soc Chem Comm 2201–2202
2. Lough AJ, Park S, Ramachandran R, Morris RH (1994) Switching on and off a new intramolecular hydrogen-hydrogen interaction and the heterolytic splitting of dihydrogen. Crystal and molecular structure of [Ir{H(η^1-SC_5H_4NH)}$_2$(PCy_3)]BF_4·2.7CH_2Cl_2. J Am Chem Soc 116:8356–8857
3. Richardson TB, deGala S, Crabtree RH, Siegbahn PEM (1995) Unconventional hydrogen bonds: intermolecular B-H…H-N interactions. J Am Chem Soc 117:12875–12876
4. Alkorta I, Blanco F, Elguero J (2010) Dihydrogen bond cooperativity in aza-borane derivatives. J Phys Chem A 114: 8457–8462
5. Yan SH, Bu YX, Cukier RI (2006) Electron bridging dihydrogen bond in the imidazole-contained anion derivatives. J Chem Phys 124:124314–124323
6. Grabowski S, Sokalski WA, Leszczynski J (2004) Nature of X-$H^{+\delta}$…$^{-\delta}$H-Y dihydrogen bonds and X-H…σ interactions. J Phys Chem A 108:5823–5830
7. Staubitz A, Robertson APM, Sloan ME, Manners I (2010) Amine- and phosphine-borane adducts: new interest in old molecules. Chem Rev 110:4023–4078
8. Staubitz A, Robertson APM, Manners I (2010) Ammonia-borne and related compounds as dihydrogen sources. Chem Rev 110: 4079–4124
9. Arunan E, Desiraju GR, Klein RA, Sadlej J, Scheiner S, Alkorta I, Clary DC, Crabtree RH, Dannenberg JJ, Hobza P, Kjaergaard HG, Legon AC, Mennucci B, Nesbitt DJ (2011) Definition of the hydrogen bond. Pure Appl Chem 83:1637
10. Sewell LJ, Lloyd-Jones GC, Weller AS (2012) Development of a generic mechanism for the dehydrocoupling of amine-boranes: a stoichiometric, catalytic, and kinetic study of H_3B NMe_2H using the $[Rh(PCy_3)_2]^+$ fragment. J Am Chem Soc 134:3598–3610
11. Cramer CJ, Gladfelter WL (1997) Ab initio characterization of $[H_3N{\cdot}BH_3]_2$, $[H_3N{\cdot}AlH_3]_2$, $[H_3N{\cdot}GaH_3]_2$. Inorg Chem 36:5358–5362
12. Guo YH, Wu H, Zhou W, Yu XB (2011) Dehydrogenation tuning of ammine borohydrides using double-metal cations. J Am Chem Soc 133:4690–4693
13. Golub IE, Gulyaeva ES, Filippov OA, Dyadchenko VP, Belkova NV, Epstein LM, Arkhipov DE, Shubina ES (2015) Dihydrogen bond intermediated alcoholysis of dimethylamine-borane in non-aqueous media. J Phys Chem A 119:3853–3868
14. Brown MP, Heseltin RW (1968) Coordinated BH_3 as a proton acceptor group in hydrogen bonding. Chem Commun 1551–1552
15. Brown MP, Heseltin RW, Smith PA, Walker PJ (1970) J Chem Soc A 410
16. Brown MP, Walker PJ (1974) Hydrogen bonds between coordinated NH_3 and BH_2 groups and OH groups. Thermodynamics of formation by infrared spectroscopy. Spectrochim Acta A 30:1125–1131
17. Merten C, Berger CJ, McDonald R, Xu YJ (2014) Evidence of dihydrogen bonding of a chiral amine-borane complex in solution by VCD spectroscopy. Angew Chem Int Edit 2014(53):9940–9943
18. O'Malley PJ (1998) Hybrid density functional studies of the oxidation of phenol-imidazole hydrogen-bonded complexes: a model for tyrosine oxidation in oxygenic photosynthesis. J Am Chem Soc 120:11732–11737
19. Yan SH, Bu YX (2004) Alteration of imidazole dimer on oxidation or water ligation. J Phys Chem B 108:13874
20. Yan SH, Bu YX (2005) Coupling properties of imidazole dimer radical cation assisted by embedded water molecule: toward understanding of interaction character of hydrogen-bonded histidine residue side-chains. J Chem Phys 122:184324–184331
21. Yan SH, Zhang L, Cukier RI, Bu YX (2007) Exploration on regulating factors for proton transfer along hydrogen-bonded water chains. Chem Phys Chem 8:944–954
22. Gutsev GL, Bartlett RJJ (1996) A theoretical study of the valence- and dipole-bound states of the nitromethane anion. J Chem Phys 105:8785–8792
23. Rienstra-Kiracofe JC, Tschumper GS, Schaefer HF III, Nandi S, Ellison GB (2002) Atomic and molecular electron affinities: photoelectron experiments and theoretical computations. Chem Rev 102:231–282
24. Ciobanu CV, Ojamae L, Shavitt I, Singer SJ (2000) Structure and vibrational spectra of $H^+(H_2O)_8$: is the excess proton in a symmetrical hydrogen bond? J Chem Phys 113:5321–5330
25. Christie RA, Jordan KD (2001) Theoretical investigation of the $H_3O^+(H_2O)_4$ cluster. J Phys Chem A 105:7551–7558

26. Mella M, Kuo JL, Clary DC, Klein ML (2005) Nuclear quantum effects on the structure and energetics of $(H_2O)_6H^+$. Phys Chem Chem Phys 7:2324–2332
27. Sychrovsky V, Grafenstein J, Cremer D (2000) Nuclear magnetic resonance spin-spin coupling constants from coupled perturbed density functional theory. J Chem Phys 113:3530–3547
28. Helgaker T, Watson M, Handy NC (2000) Analytical calculation of nuclear magnetic resonance indirect spin-spin coupling constants at the generalized graient approximation and hybrid levels of density-functional theory. J Chem Phys 113:9402–9409
29. Sychrovsky V, Sponer J, Hobza P (2004) Theoretical calculation of the NMR spin−spin coupling constants and the NMR shifts allow distinguishability between the specific direct and the water-mediated binding of a divalent metal cation to guanine. J Am Chem Soc 126:663–672
30. Wolinski K, Hinton JF, Pulay P (1990) Efficient implementation of the gauge-independent atomic orbital method for NMR chemical shift calculations. J Am Chem Soc 112:8251–8260
31. Cheeseman JR, Trucks GW, Keith TA, Frisch MJ (1996) A comparison of models for calculating nuclear magnetic resonance shielding tensors. J Chem Phys 104:5497–5509
32. Ramsey NF (1953) Electron coupled interactions between nuclear spins in molecules. Phys Rev 91:303–307
33. Frisch MJ, Trucks GW, Schlegel HB, Scuseria GE, Robb MA, Cheeseman JR, Scalmani G, Barone V, Mennucci B, Petersson GA, Nakatsuji H, Caricato M, Li X, Hratchian HP, Izmaylov AF, Bloino J, Zheng G, Sonnenberg JL, Hada M, Ehara M, Toyota K, Fukuda R, Hasegawa J, Ishida M, Nakajima T, Honda Y, Kitao O, Nakai H, Vreven T, Montgomery JA, Peralta JE Jr, Ogliaro F, Bearpark M, Heyd JJ, Brothers E, Kudin KN, Staroverov VN, Keith T, Kobayashi R, Normand J, Raghavachari K, Rendell A, Burant JC, Iyengar SS, Tomasi J, Cossi M, Rega N, Millam JM, Klene M, Knox JE, Cross JB, Bakken V, Adamo C, Jaramillo J, Gomperts R, Stratmann RE, Yazyev O, Austin AJ, Cammi R, Pomelli C, Ochterski JW, Martin RL, Morokuma K, Zakrzewski VG, Voth GA, Salvador P, Dannenberg JJ, Dapprich S, Daniels AD, Farkas O, Foresman JB, Ortiz JV, Cioslowski J, Fox DJ (2010) Gaussian 09, revision B.01; Gaussian Inc, Wallingford
34. Rao BK, Jena P, Burkart S, Gantefor G, Seifert G (2001) AlH_3 and Al_2H_6: magic clusters with unmagical properties. Phys Rev Lett 86: 692–695
35. Kar T, Scheiner S (2003) Comparison between hydrogen and dihydrogen bonds among H_3BNH_3, H_2BNH_2, and NH_3. J Chem Phys 119:1473–1482
36. Li JS, Zhao F, Jing FQ (2002) B-$H^{\delta-}$ σ bond as dihydrogen bond acceptor: some theoretical observations and predictions. J Chem Phys 116:25–32
37. Patwari GN, Ebata T, Mikami N (2002) Dihydrogen bonded phenol-borane-dimethylamine complex: an experimental and theoretical study. J Chem Phys 116:6056–6063
38. Patwari GN, Ebata T, Mikami N (2001) Gas phase dihydrogen bonded phenol-borane-trimethylamine complex. J Chem Phys 114:8877–8879
39. Wu D, Li Y, Li Z, Chen W, Li ZR, Sun CC (2006) Characterization of solvated electrons in hydrogen cyanide clusters: $(HCN)_n^-$ (n = 3, 4). J Chem Phys 124:054310–054319
40. Monde K, Miura N, Hashimoto M, Taniguchi T, Inabe T (2006) Conformational analysis of chiral helical perfluoroalkyl chains by VCD. J Am Chem Soc 128:6000–6001
41. Hopmann KH, Sebestik J, Novotna J, Stensen W, Urbanova M, Svenson J, Svendsen JS, Bour P, Ruud K (2012) Determining the absolute configuration of two marine compounds using vibrational chiroptical spectroscopy. J Org Chem 77:858–869
42. Merten C, Hiller K, Xu Y (2012) Effects of electron configuration and coordination number on the vibrational circular dichroism spectra of metal complexes of trans-1, 2-diaminocyclohexane. Phys Chem Chem Phys 14:12884–12891
43. Merten C, Reuther JF, Desousa JD, Novak BM (2014) Identification of the specific, shutter-like conformational reorientation in a chiroptical switching polycarbodiimide by VCD spectroscopy. Phys Chem Chem Phys 14:11456–11460